https://doi.org/10.5194/egusphere-2025-2645
Preprint. Discussion started: 22 July 2025

Cloud Base Height Determines Fog Occurrence Patterns in the Namib Desert and Can Be Estimated from Near-Surface Relative Humidity

Deepanshu Malik[1,2], Hendrik Andersen[1,2], Jan Cermak[1,2], Roland Vogt[3], and Bianca Adler[4,5]

[1]Institute of Photogrammetry and Remote Sensing, Karlsruhe Institute of Technology (KIT), Karlsruhe, Germany
[2]Institute of Meteorology and Climate Research Atmospheric Trace Gases and Remote Sensing, Karlsruhe Institute of Technology (KIT), Karlsruhe, Germany
[3]Department of Environmental Sciences, University of Basel, Basel, Switzerland
[4]Cooperative Institute for Research in Environmental Sciences (CIRES), University of Colorado Boulder, Boulder, Colorado, USA
[5]NOAA Physical Sciences Laboratory, Boulder, Colorado, USA

Correspondence: Deepanshu Malik (deepanshu.malik@kit.edu) and Hendrik Andersen (hendrik.andersen@kit.edu)

Abstract. In the hyper-arid Namib Desert, fog serves as the only regular source of moisture, vital for sustaining local ecosystems. While fog occurrence in the region is typically associated with the advection of marine stratus clouds and their interaction with topography, its spatial distribution is strongly influenced by cloud base height, which remains poorly understood. To address this gap, this study utilizes ground-based remote sensing and in-situ observations to analyze systematic spatial and temporal patterns of cloud base height. Our results reveal clear seasonality and a diurnal cycle, with cloud base lowering moderately (10–50 m h^{-1}) during the evening and early night, and lifting rapidly (30–150 m h^{-1}) after sunrise, especially inland. A strong and consistent negative correlation (r ≈ -0.75) between cloud base height and near-surface relative humidity was identified using quantile regression, enabling accurate cloud base height estimation with a mean absolute error of 46 m and a mean absolute percentage error of 19 % relative to ground-based measurements. In a case study, the potential value of the estimated cloud base height for separating fog from low clouds in satellite-based products is shown. In the future, a full integration of the estimated cloud base height with a satellite-based fog and low-cloud product can enable a spatially continuous mapping of fog in the region for the first time, which would facilitate fog ecological impact studies.

1 Introduction

Fog is a characteristic meteorological phenomenon in the Namib Desert, one of the driest regions on Earth, which lies along the southwestern coast of Africa, and serves a critical function in supplying moisture to the desert's ecosystems. It thereby supports the persistence of plant and animal life in this otherwise arid environment (e.g. Seely and Henschel, 1998; Shanyengana et al., 2002; Ebner et al., 2011; Azúa-Bustos et al., 2011; Roth-Nebelsick et al., 2012; Eckardt et al., 2013; McHugh et al., 2015). An example of this is the existence of fertile islands of vegetation, known as "Fog-Plant-Oases" (Gan et al., 2024), which depend on fog deposition for their water supply. In addition, fog can transport nutrients and pollutants (Weathers et al., 2020),

https://doi.org/10.5194/egusphere-2025-2645
Preprint. Discussion started: 22 July 2025

potentially impacting biogeochemistry where fog water is deposited (Warren-Rhodes et al., 2013; Gottlieb et al., 2019). In light of expected regional climatic changes in southern Africa (warmer and drier, (Maúre et al., 2018)), Namib fog could become even more important to regional ecosystems in the future.

The Namib Desert experiences fog throughout the year; however, historical station observations (Nagel, 1959; Lancaster et al., 1984) and more recent data from the FogNet observation stations (Andersen et al., 2019) show a clear seasonal variation in spatial fog occurrence patterns. These patterns are closely related to the distance from the coast, the elevation of the land surface, and the seasonally varying vertical position of the low stratus layer. Fog in the Namib Desert is predominantly of advective nature (Olivier and Stockton, 1989; Seely and Henschel, 1998; Andersen et al., 2019; Spirig et al., 2019; Formenti et al., 2019; Andersen et al., 2020), with advection fog frequently occurring in a narrow coastal area (less than 15 km) and an advected stratus cloud often extending further inland, historically referred to as "advective fog" and "high fog" respectively in (Seely and Henschel, 1998). This advected stratus layer is typically lower-lying (≈ 200 m AMSL, referred to as the "Low-FLC Season", Andersen et al. (2019)) during the austral winter, but during the austral summer, it rises to around 400 m AMSL (referred to as the "High-FLC Season", Andersen et al. (2019)) and can extend more than 60 km inland, where it may intercept the terrain and manifest as fog (Olivier, 1992; Andersen et al., 2019). These spatio-temporal patterns of the advected fog and low stratus clouds can be observed using satellites (Olivier, 1995; Cermak, 2012; Andersen and Cermak, 2018; Andersen et al., 2019). However, distinguishing fog from other very low-lying stratiform clouds in satellite images is very challenging and not conclusively solved (Cermak and Bendix, 2011; Egli et al., 2018). While studies by Cermak (2018) and Qiao et al. (2022) highlight the potential of satellite-based lidar observations for fog detection, the data's sparse coverage limits its suitability for continuous spatiotemporal fog mapping. As in advected stratus situations, the stratus base frequently does not reach the surface near the lower-lying coastal areas (Andersen et al., 2019), the vertical position of the stratus layer is a critical parameter that partially determines fog occurrence patterns. So far, only the seasonal cycle of the cloud base has been analyzed with sparsely available ground-based remote sensing data. Diurnal vertical developments during the fog and low cloud (FLC) life cycle, such as cloud base lowering after the stratus is advected inland and stratus lifting in the fog dissipation phase, have only been documented for a small number of cases (Spirig et al., 2019).

This study aims to address this gap by analyzing cloud base height (CBH) measurements from multiple ceilometers across a transect from the coast to inland locations. This study seeks to document typical seasonal and diurnal CBH patterns, and to investigate the potential of using local in-situ measurements of surface relative humidity (RH) to estimate CBH with a statistical model. Since marine stratus and coastal stratocumulus clouds typically develop within a well-mixed boundary layer (Wood and Bretherton, 2004), a strong correlation between near-surface RH and CBH is expected. Given that RH measurements are available at more locations for a longer time period, this approach could be used to generate a continuous, long-term dataset of estimated CBH across the range of FogNet stations. Our research aims to answer the following key questions:

1. What are the patterns of CBH development during the FLC life cycle, and do they vary with coastal proximity and season?

2. Can local station measurements of RH be used to accurately estimate CBH of FLCs?

https://doi.org/10.5194/egusphere-2025-2645
Preprint. Discussion started: 22 July 2025

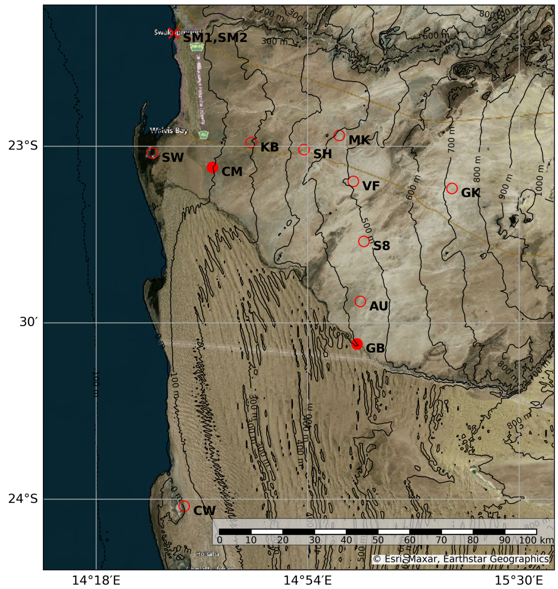

Figure 1. Map showing the research area in the central Namib and the spatial distribution of the FogNet stations described in Table 1. The stations marked with filled red dots (GB:Gobabeb and CM:Coastal Met) and at Swakopmund (SM1 and SM2, marked as X, not a part of FogNet) are equipped with ceilometers, providing continuous CBH observations.

2 Data and Methods

2.1 The study region: The Central Namib

The Central Namib Desert, particularly the area monitored by the FogNet station network (Kaspar et al., 2015) (≈ 22.5°–24° S and 14°–15.5° E, Figure 1), is a focal point for investigating FLCs due to their high frequency of occurrence (Andersen et al., 2019) and historical station measurements (Nagel, 1959; Lancaster et al., 1984). The cold Benguela ocean current along the coast of the Namib Desert facilitates the formation of extensive low-level stratus clouds over the ocean (Andrews and Hutchings, 1980), which often advect eastward after sunset. To the east, near Gobabeb, the terrain rises up to 406 m for 56 km inland distance, intercepting the advected stratus clouds to form fog where CBH reaches the surface. Only rarely, fog occurs further inland than 100 km (Olivier, 1992), or ≈ 15°30'E in the region shown in Figure 1.

2.2 Ceilometer measurements

For this study, ceilometer data were sourced from two key instruments deployed in the Central Namib region (Figure 1): the Vaisala CL31 at Coastal Met (CM) and Swakopmund (SM), and the Campbell Scientific CS135 at Gobabeb (GB). Ceilometers, which require regular maintenance and cleaning of their optical screens, face unique challenges in harsh desert environments like Namibia. The combination of extreme conditions and infrequent maintenance, together with other technical issues, has

https://doi.org/10.5194/egusphere-2025-2645
Preprint. Discussion started: 22 July 2025

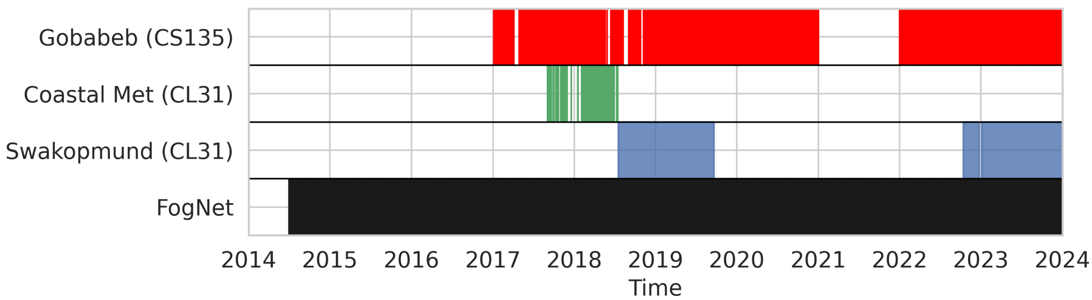

Figure 2. Temporal coverage of ceilometer (CL31 and CS135) and in-situ meteorological (FogNet) data used in this study across key locations in the Central Namib.

led to substantial data gaps. Despite these challenges, data availability at Gobabeb has remained relatively consistent, largely due to regular maintenance efforts, providing a valuable and continuous record. The temporal availability of ceilometer data from these locations is illustrated in Figure 2. Notably, the CL31 at Swakopmund was repositioned by ≈500 m towards the coast in 2022. The CL31 ceilometer, utilizing a 910 nm InGaAs laser diode, offers a vertical resolution of 10 m and a temporal resolution of 20 s (as documented in instrument CL31-2 in (Weigner et al., 2019; Vaisala, 2024). The manufacturer specifies a range accuracy of approximately ±5 m. In comparison, the CS135 ceilometer operates at a 905 nm wavelength and provides a higher vertical resolution configurable to 5 m, with a target range accuracy of ±4.6 m for ranges up to 10 km (Barbato et al., 2016; CampbellScientific, 2018). This enhanced resolution allows for even more detailed profiling of the vertical structure of the atmosphere at each 30 s interval. It should be noted that CBH derived from attenuated backscatter can vary between different ceilometer types due to differing firmware definitions, with differences of approximately 50–100 m for liquid water clouds (Preissler et al., 2024). Both CL31 and CS135 instruments have blind zones (i.e., regions within 3 % overlap, corresponding to a 97 % correction but still allowing for cloud base detection) at 10 m and 40 m, respectively. However, more robust detection, defined as 50 % optical overlap, occurs at approximately 40 m for the CL31 and 250 m for the CS135 (Preissler et al., 2024). To balance measurement reliability with suitability for detecting low clouds and fog events, we use 40 m as the minimum CBH detection limit. To focus exclusively on FLCs, CBH values exceeding 1000 m are excluded from the dataset. While ceilometers are reliable instruments for vertical atmospheric profiling, it is important to note that they are typically not calibrated against one another. Consequently, small biases may occur between measurements from identical instruments, as discussed in (Weigner et al., 2019). All measurements were recorded using Campbell Scientific data loggers, which were further processed by LoggerNet software (data acquisition software) into .dat files (CampbellScientific, 2007).

2.3 FogNet station data

In addition to ceilometer data, this study incorporates meteorological observations from the FogNet network (Kaspar et al., 2015). FogNet comprises a network of meteorological stations strategically positioned along two transects (N-S, and W-E) (as

https://doi.org/10.5194/egusphere-2025-2645
Preprint. Discussion started: 22 July 2025

Table 1. Latitude, longitude, elevation, and distance to the coast of the FogNet stations, sorted from west to east. Station positions are shown in Figure 1.

Station (west to east)	Latitude (°S)	Longitude (°E)	Elevation (m AMSL)	Distance to coast (km)
Saltworks (SW)	–23.02	14.46	5	4
Conception Water (CW)	–24.02	14.55	10	10
Coastal Met (CM*)	–23.06	14.63	94	17
Kleinberg (KB)	–22.99	14.74	185	24
Sophies Hoogte (SH)	–23.01	14.89	342	40
Marble Koppie (MK)	–22.97	14.99	419	51
Vogelfederberg (VF)	–23.10	15.03	515	58
Gobabeb (GB*)	–23.56	15.04	406	56
Aussinanis (AU)	–23.44	15.05	444	55
Station 8 (S8)	–23.27	15.06	490	55
Garnet Koppie (GK)	–23.12	15.31	733	85
Swakopmund1** (SM1*)	-22.68	14.52	3	0.05
Swakopmund2** (SM2*)	-22.68	14.53	15	1

*Stations with ceilometers installed.
**Station not a part of FogNet network.

shown in Figure 1, with further details on the individual stations provided in Table 1). The stations measure fog precipitation (measured using the Juvik fog collector (Juvik and Nullet, 1995)), temperature and humidity (Campbell Scientific CS215 sensor (CampbellScientific, 2013b)), wind speed and direction (R.M Young Model 05103 Wind Monitor (CampbellScientific, 2013a)), net radiation (CNR4 Net Radiometer (CampbellScientific, 2017)), and other meteorological variables. These observations offer valuable insights into the characteristics related to the occurrence of fog and low clouds (Spirig et al., 2019). Notably, the availability of these meteorological datasets has been consistent over about a decade, with data available since 2014-07-01, as illustrated in Figure 2. While short-term outages may occur occasionally, the overall data coverage remains reliably continuous.

2.4 FLC Satellite Product

Monitoring fog and low cloud cover in regions with sparse observational networks, such as the Namib Desert, requires reliable remote sensing techniques. This study employs a satellite-based fog and low cloud (FLC) product (Andersen and Cermak, 2018) that is based on Spinning Enhanced Visible and Infrared Imager (SEVIRI) observations mounted on the geostationary Meteosat Second Generation (MSG) satellites. By making use of thermal infrared observations, FLCs can be detected during day and night at the native 15 min and 3 km (at nadir) resolutions. The validation against surface net radiation measurements has shown a high accuracy, with a 97 % correctness of the classifications and a false alarm rate of 12 %. The FLC product has previously been used to study the spatio-temporal patterns of FLC occurrence (Andersen et al., 2019), as well as FLC processes

https://doi.org/10.5194/egusphere-2025-2645
Preprint. Discussion started: 22 July 2025

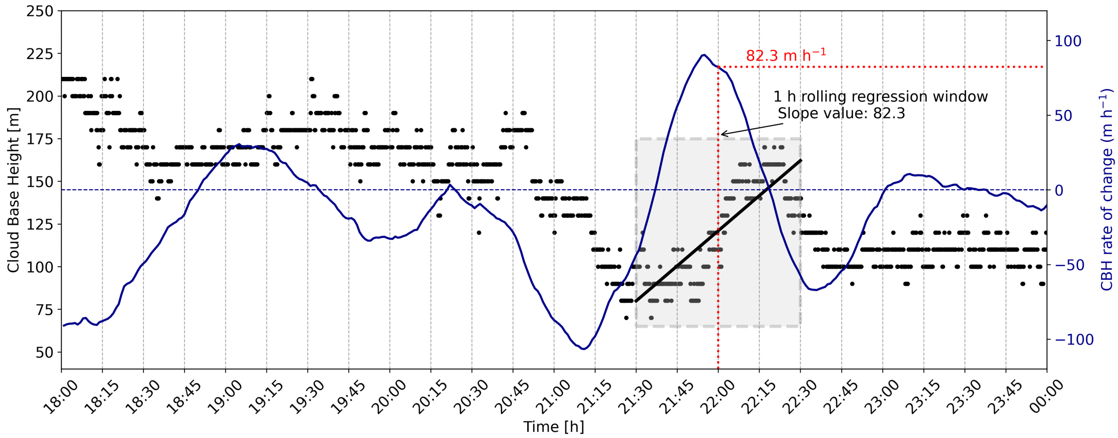

Figure 3. Illustration of the 1 h rolling regression method applied to 1 min resolution CBH data. Black dots denote individual CBH measurements; the blue line shows the computed CBH rate of change (m h^{-1}). The shaded region indicates the 1-hour regression window centered around the 22:00 h timestep. The slope of the fitted black line within this window corresponds to the rate of CBH change at 22:00 h

(Andersen et al., 2020; Mass et al., 2024). However, note that this satellite-based method is not able to differentiate between fog and low clouds, a general limitation of fog retrievals from satellite imagers.

2.5 Estimation of FLC lowering/lifting rates

To gain deeper insights into CBH dynamics during FLC events, this study estimates CBH lowering and lifting rates using a rolling regression approach (Zivot and Wang, 2003). To mitigate short-term fluctuations and enhance the robust quantification of lowering and lifting phases in the raw CBH data, which is resampled at a 1 min resolution, a 1 h rolling window is applied. This window length balances sensitivity and stability, preserving sufficient temporal resolution to capture gradual CBH variations. Within each 1 h window, a linear regression is performed to compute the slope of the CBH trend, representing the rate of change in CBH. Positive slopes indicate a lifting of the cloud base, while negative slopes signify a lowering. This approach yields a continuous time series of average hourly CBH rate of change (m h^{-1}) at a 1 min temporal resolution. Figure 3 illustrates the methodology, showing a 1 h rolling regression applied to CBH data. The shaded region marks an exemplary regression window, with the slope of the fitted black line representing the CBH rate of change at the center timestep, in this case, a lifting event with a slope of 82.3 m h^{-1} at 22:00 h. This example demonstrates the method's capacity to capture underlying CBH trends while minimizing short-term variability. To further analyze diurnal patterns in CBH dynamics, the computed CBH rates are first resampled to hourly averages and then grouped by hour of the day across all days, months, and years. This resampling provides a structured view of the diurnal evolution of CBH changes and facilitates the quantification of the number of lifting and lowering events within each hourly interval during the observational period.

https://doi.org/10.5194/egusphere-2025-2645
Preprint. Discussion started: 22 July 2025

2.6 CBH Estimation from FogNet Station Measurements

Due to the sparsity of ceilometer measurements in the Central Namib region, this study explores the potential of using local station measurements from the FogNet network to estimate CBH. RH is used to predict CBH using a quantile (0.5) regression model (Koenker and Hallock, 2001). Quantile regression is employed to model the conditional distribution of a predictand at different quantiles. Unlike Ordinary Least Squares regression (OLS), which models only the conditional mean, quantile regression allows for the estimation of CBH across various percentiles, thereby accounting for, offering advantages over OLS regression by capturing the full distributional behavior of the response, particularly in the presence of heteroscedasticity or non-normal residuals. Unlike OLS, which minimizes the squared residuals to estimate the conditional mean, quantile regression minimizes the *quantile loss function*:

$$L_\tau(u) = u\left(\tau - \mathbb{I}_{(u<0)}\right) \tag{1}$$

where $u = y - f(x)$ is the residual, τ is the target quantile (here, 0.5), and $\mathbb{I}$ is the indicator function (equal to 1 if $u < 0$, and 0 otherwise). This loss function yields estimates that are more robust to outliers and skewed distributions, which are common in CBH and RH dataset. To illustrate the method, consider a simplified example where RH measurements (%) are used to estimate CBH (m) at a single station. Suppose a quantile regression model of the form

$$\mathrm{CBH} = \beta_0 + \beta_1 \cdot \mathrm{RH} \tag{2}$$

is fitted to the data, yielding coefficients $\beta_0 = 500$ and $\beta_1 = -22$. This implies that the median CBH decreases by 22 m for every 1% increase in RH, consistent with the physical expectation that higher RH correlates with lower cloud bases. The model thereby captures the central tendency of the CBH–RH relationship while accounting for data asymmetry and variability.

Leveraging the continuous RH data available from FogNet stations, this approach aims to generate extended time series of estimated CBH (CBH_e), even in the absence of direct ceilometer measurements. To assess regional consistency of the CBH-RH relationship, CBH is regressed upon RH individually for the Coastal Met and Gobabeb stations.

3 Results and Discussion

3.1 Diurnal and Seasonal Patterns of CBH

Diurnal and seasonal patterns of CBH and their variability across the three ceilometer locations are shown in Figure 4. Each panel displays seasonal variation along the horizontal axis (month) and diurnal variation along the vertical axis (hour of day - centered on midnight as FLCs occur during the night/early morning). For a comprehensive comparison, we analyze each row across columns, highlighting spatial differences in CBH behavior.

The first row of Figure 4 illustrates the diurnal and seasonal patterns of mean CBH above ground level (AGL) for each location. At Swakopmund, the diurnal variation in CBH is not as clearly pronounced as the seasonality, likely due to frequent advection fog forming at the surface, which often attenuates the ceilometer signal. Additionally, the persistent marine boundary

https://doi.org/10.5194/egusphere-2025-2645
Preprint. Discussion started: 22 July 2025

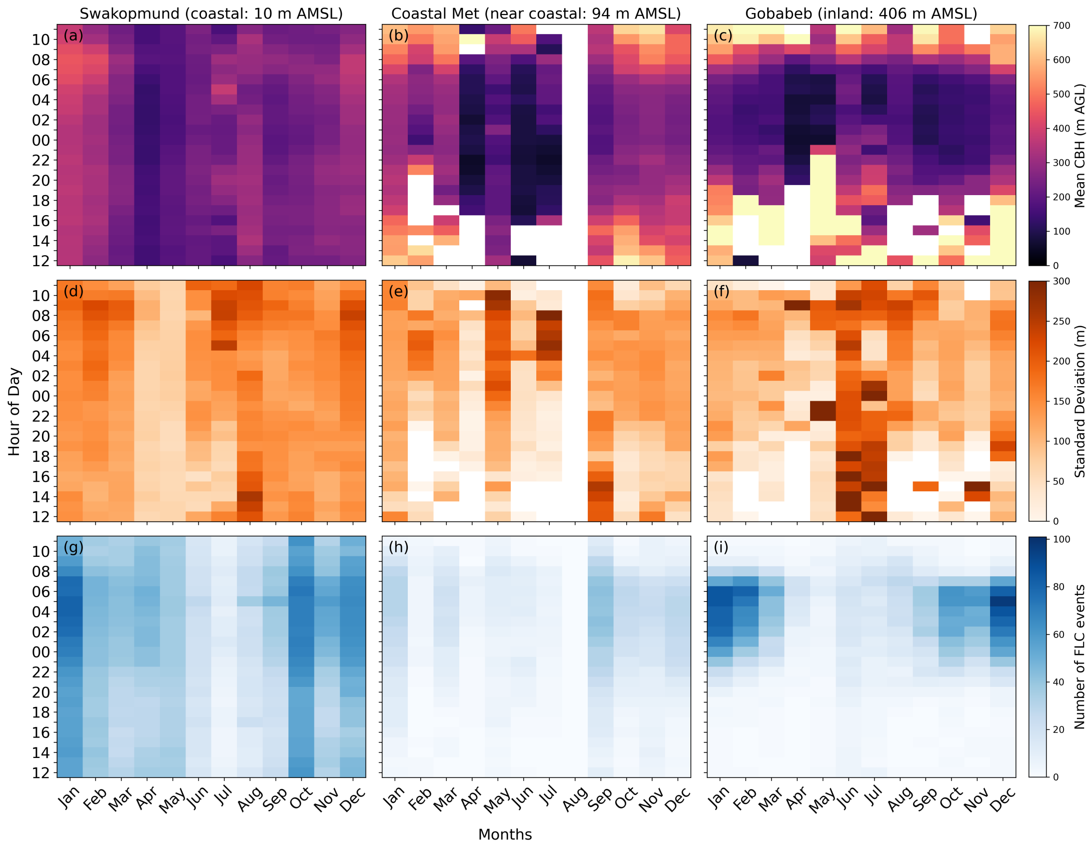

Figure 4. Diurnal and seasonal variations in CBH statistics at Swakopmund (left column), Coastal Met (middle column), and Gobabeb (right column).The first row (a–c) shows the mean CBH above ground level, the second row (d–f) presents the standard deviation of mean CBH, and the third row (g–i) indicates the number of FLC events on which the statistics are based. The x-axis denotes the months of the year, while the y-axis corresponds to the time (hour of the day, UTC).

layer contributes to stable atmospheric conditions throughout the day and night. This contrasts sharply with Coastal Met and Gobabeb, where distinct diurnal fluctuations are evident. At these near-coast and inland locations, mean CBH is typically lower during the nighttime, aligning with the occurrence of nocturnal fog. Seasonal variations in mean CBH are evident at all three locations, though their prominence varies. These seasonal variations are more pronounced at inland sites, where CBH fluctuations are greater compared to the more stable conditions near the coast. At Swakopmund and Coastal Met, the lowest mean CBH values are observed during April, May, and June, coinciding with the "Low-FLC season". During this period, mean CBH is relatively higher at Swakopmund than at Coastal Met, suggesting that the advected stratus layer resides at around 150 m AGL at Swakopmund (10 m AMSL) and below 100 m AGL at Coastal Met (94 m AMSL). However, Gobabeb follows a similar but extended seasonal pattern, with the lowest CBH values peaking from April to November. The predominant period

https://doi.org/10.5194/egusphere-2025-2645
Preprint. Discussion started: 22 July 2025

occurs from September to November, coincides with the "High-FLC season", when cloud events reaching inland are more frequent. The relatively lower mean CBH values at Gobabeb during April and May may also reflect sampling limitations, as only a few FLC events are detectable inland during this period. At both Coastal Met and Gobabeb, fog formation occurs as advected stratus clouds interact with the local topography, though this process is seasonally distinct, prevailing in the Low-FLC season near the coast and in the High-FLC season inland (Andersen et al., 2019). The seasonal differences in CBH patterns between coastal and inland stations emphasize the spatial extent of the cloud deck across the Namib Desert. However, in this analysis, a direct comparison of CBH above mean sea level across the stations, which could offer clearer insight into the vertical structure of the cloud field, is limited by differing observational periods and associated sampling inconsistencies. The second row (Figure 4 (d,e,f)) displays the standard deviation of CBH, providing insights into the variability of mean CBH across locations. Swakopmund exhibits fairly consistent low CBH variability throughout the year. While in Coastal Met and Gobabeb there is a higher variability during austral winter. However, these statistics are also based on a very limited amount of FLC events. The last row of Figure 4 (g,h,i) provides important context regarding the number of FLC events (days) contributing to the presented CBH statistics, which is driven by both the frequency of cloud events during each hour and month and the measurement times. Data availability (Figure 2) at Coastal Met experiences significant data gaps due to its limited observational period, which is reflected in the number of FLC events recorded. However, at Swakopmund and Gobabeb, data availability remains relatively stable throughout the year, ensuring a consistent representation of FLC events. Additionally, Gobabeb exhibits a reduced number of FLC events during the austral winter (AMJ), when FLC typically do not reach far inland (Andersen et al., 2019). This also suggests a selection bias in the calculated statistics, as only higher-level FLCs are observed inland at Gobabeb. Overall, the spatial differences in CBH observed in Figure 4 underscore the interplay of coastal influence, atmospheric stability, and topographical effects in shaping the diurnal and seasonal variability of CBH across the Namib Desert region.

3.2 Fog Life Cycle

In this section, CBH patterns are analyzed across the fog life cycle, encompassing the stages of initial occurrence, maturity, and dissipation. Figure 5 presents observational evidence of these stages during a fog event at Coastal Met (31-01-2018). The Figure 5(a) presents a time-height cross-section of backscatter intensity (measured in $sr^{-1}\ m^{-1}$) with overlying CBH markers (black), visualizing the vertical position of the cloud layer over time. At the onset of the event, a stratiform cloud layer is detected at approximately 300 m altitude (AGL) and begins descending after sunset, exhibiting intermittent lifting and lowering but then settling in at a CBH of less than 100 m above ground. High backscatter intensity was detected already at 40 m above ground (the detection limit of the CL31) indicating reduced visibility below the detected cloud base. During this phase, RH exceeded 95%, and fog precipitation (blue dots) was recorded, as shown in Figure 5(c). These conditions persisted until a few hours after sunrise, when the dissipation phase began, characterized by a rapid rise in CBH.

To investigate CBH vertical dynamics, the rate of CBH change was computed using a rolling 1 h regression slope method (detailed in Section 2.5), as shown in the middle panel of Figure 5(b). Positive values (green) indicate CBH lifting, while negative values (red) correspond to CBH lowering. The grey-shaded background represents the hourly mean with the interquartile

https://doi.org/10.5194/egusphere-2025-2645
Preprint. Discussion started: 22 July 2025

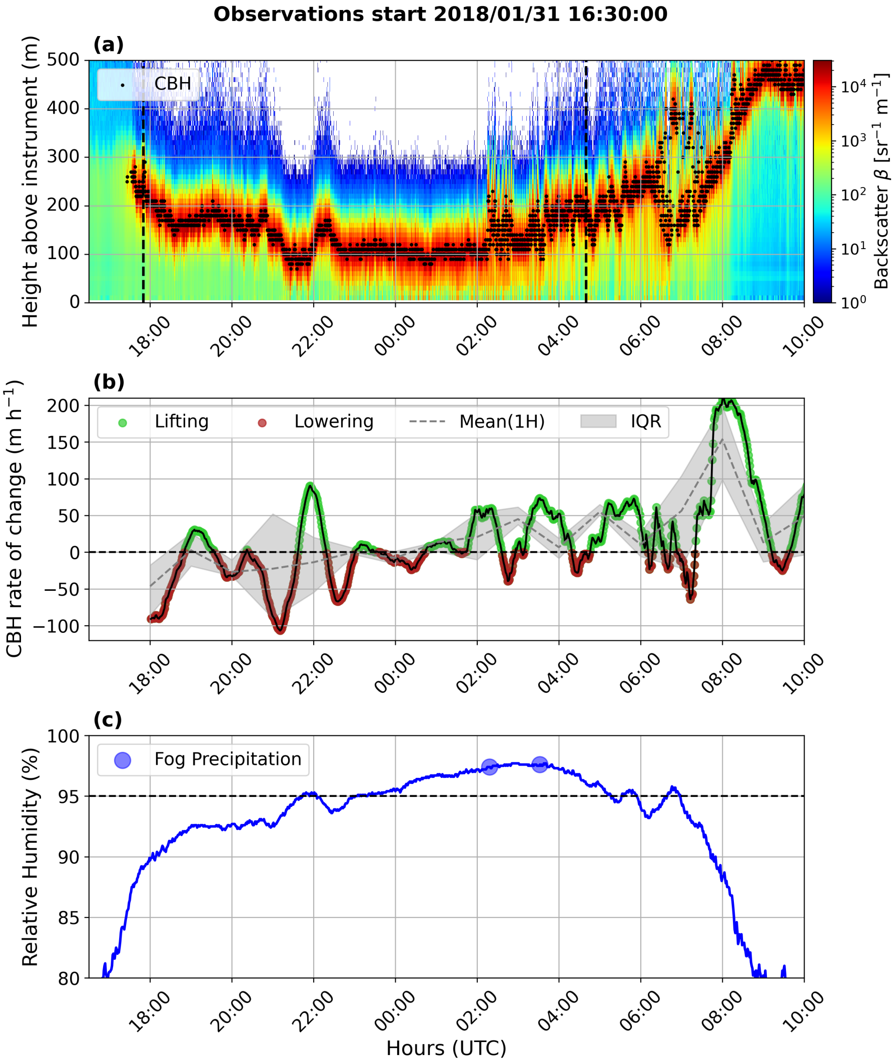

Figure 5. Time series analysis of the fog life cycle at the Coastal Met station on 31-01-2018. (a) Backscatter intensity (sr^{-1} m^{-1}) with CBH markers, illustrating fog evolution. Dashed lines indicate the times of sunrise and sunset. (b) CBH rates of change ($m\ h^{-1}$) with lifting (green) and lowering (red), alongside the hourly mean (dashed) and interquartile range (shaded). (c) RH (%) with fog precipitation indicated by blue markers. The figure captures key phases of fog occurrence, development, and dissipation.

range, providing a smoothed depiction of CBH variations by filtering short-term fluctuations. In the early hours after sunset, consistent negative values reflect a gradual descent of the advected cloud layer. This transition is followed by large positive values after sunrise, indicative of rapid lifting. This case illustrates that the vertical evolution of Namib fog during its life cycle can feature considerable variability and that this variability can be captured well by the estimated CBH change rates.

https://doi.org/10.5194/egusphere-2025-2645
Preprint. Discussion started: 22 July 2025

3.2.1 Diurnal Evolution

To assess whether the CBH dynamics observed in the case study are representative of broader FLC patterns, the rate of change in CBH was computed for all observed FLC events. The diurnal variations in CBH rates across all three stations and different seasons are presented in Figure 6. The sample size displayed for each hour and station provides insight into the frequency of FLC events as well as the robustness of the statistics presented. CBH statistics are reported only for hours where the sample size exceeds five, ensuring that the results are representative of the prevailing conditions. During both seasons, FLCs exhibit a similar diurnal pattern of constant CBH or moderate lowering (up to -50 m h^{-1} in some cases) during the evening and early night, transitioning to near-zero or slightly fluctuating values during the night that signify a gradual lowering of CBH followed by a constant cloud base altitude. However, after sunrise, a pronounced increase in the CBH rate of change (up to +150 m h^{-1}) is observed, with the most rapid CBH lifting occurring between 08:00 and 10:00 UTC. The diurnal CBH variations are stronger during the austral summer when CBH is typically higher. This suggests that the lowering and lifting of advected stratus clouds may be common mechanisms for fog formation and dissipation, respectively, and points to the influence of stronger solar forcing during the austral summer to a faster lifting of FLCs in the morning. One should note that already in the hours before sunrise, FLCs experience a moderate lifting that is mostly below 10 m h^{-1}. The CBH diurnal cycle is shown to be strongly dependent on coastal proximity, as in Swakopmund CBH is nearly constant throughout the day (only moderately lifting after sunrise during austral summer). In contrast, CBH lifting rates are between 50 and 100 m h^{-1} in Coastal Met, and even more pronounced in Gobabeb where lifting rates exceed 100 m h^{-1} during austral summer. These findings suggest that the distance from the coast significantly influences fog dissipation dynamics. The computed CBH change rates in this study are consistent with previously documented CBH lowering rates associated with fog formation $\sim$ 40–60 m h^{-1} (Dupont et al., 2016; Fathalli et al., 2022; Singh et al., 2024), and CBH lifting during fog dissipation (Wærsted et al., 2019; Toledo et al., 2021; Dione et al., 2023).

3.2.2 Possible Processes

The analysis indicates that stratus lowering is a common fog formation mechanism during the High-FLC season (August-March) Figure 6(b) and case study in Figure 5. In the Low-FLC season (April-July) Figure 6(a), fog formation is less linked to lowering cloud bases, likely due to generally lower cloud heights, with fog primarily resulting from the interaction of stratus with topography. Across both seasons, fog dissipation appears to be predominantly driven by stratus lifting. To date, no study has specifically examined the underlying processes of stratus lowering in this region. Nevertheless, research conducted in other regions provides insights into the mechanisms that can contribute to stratus lowering. Stratus lowering is primarily driven by the evaporation of cloud droplets below the cloud base, which cools and moistens the sub-cloud layer. This process can occur either through turbulent mixing where droplets are transported downward by eddies generated by strong cloud-top cooling (Pilié et al., 1979; Dupont et al., 2012; Wagh et al., 2021; Fathalli et al., 2022; Singh et al., 2024), or through gravitational settling when droplets grow large enough to fall out of the cloud (Dupont et al., 2012; Pope and Igel, 2024). Unlike regions such as Central Europe, where stratus lowering frequently occurs under quasi-stationary cloud conditions, the Namibian stratus

https://doi.org/10.5194/egusphere-2025-2645
Preprint. Discussion started: 22 July 2025

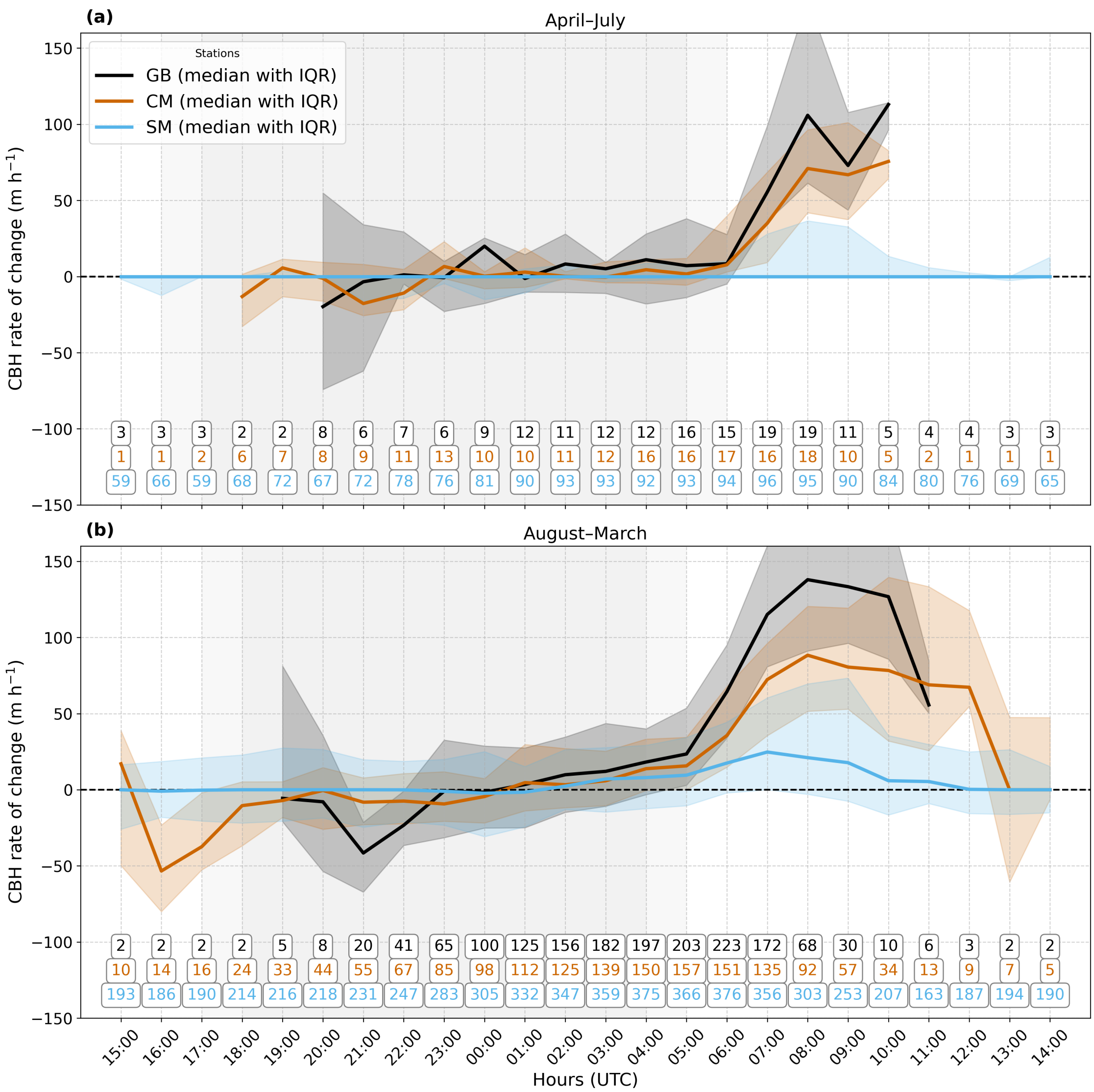

Figure 6. Hourly variation in the CBH rate of change (m h^{-1}) for three stations (GB, CM, SM) during (a) the Low-FLC season (April–July) and (b) the High-FLC season (August–March). Solid lines indicate the median, while shaded regions represent the interquartile range (IQR). Positive values correspond to CBH lifting, whereas negative values indicate lowering. Sample sizes for each station and hour are indicated by numbers; however, the CBH rate of change is only displayed for hours with a sample size greater than five.

is subject to significant advection. This raises the possibility that the observed CBH lowering and lifting in the Namib could also be influenced by the geometry of the advected stratus. One potential factor is the presence of a spatial gradient in cloud thickness, where e.g. differential advection speeds between the cloud top and base could create a sheared cloud edge. Such a process might contribute to variations in CBH rate of change, suggesting that cloud geometry and advection dynamics

https://doi.org/10.5194/egusphere-2025-2645
Preprint. Discussion started: 22 July 2025

could play an important role in modulating CBH evolution and, in extension, fog occurrence and dissipation in the region. The time of the onset and peak of the lowering phase at Coastal Met and Gobabeb in Figure 6(b) correspond to the typical start of the FLC life cycle at these locations (Andersen and Cermak, 2018; Andersen et al., 2019), and the temporal delay in lowering is indicative of an increasingly thick stratus that is advected over these locations. Considering the distance between these locations would yield an estimated average advection speed of $\approx$2.5 m h^{-1}. Furthermore, our analysis extends this perspective by capturing the stratus lifting rates of up to 150 m h^{-1} indicating that fog events predominantly dissipate as the fog layer rapidly ascends into a stratus cloud deck following sunrise (Wærsted et al., 2019; Toledo et al., 2021; Dione et al., 2023). This dissipation is likely driven by multiple factors, including enhanced evaporation at the cloud base, which induces a decoupling between the surface and the cloud layer (Dupont et al., 2012), a pronounced increase in surface wind speed and turbulence kinetic energy, and a shift toward slightly warmer near-surface air temperatures (Singh et al., 2024), all of which contribute to cloud base lifting and, consequently, fog dissipation. Moreover, the stronger lifting rates observed at inland stations in Figure 6 may result from several interconnected processes. First, inland locations such as Gobabeb may at times be embedded within the cloud layer, potentially positioning them closer to the cloud top. Due to the thinner stratus layer overhead, more solar radiation can penetrate to the surface, leading to enhanced surface heating. This, in turn, accelerates the deepening of the planetary boundary layer and promotes the lifting of the entire cloud layer. Figure 7 provides empirical support for the proposed mechanism by comparing cumulative net radiation and CBH evolution at Gobabeb and Coastal Met, considering only nights with cloud presence at both sites. This ensures a realistic comparison under FLC conditions. Although the analysis is limited to the October–December 2017 period due to data availability, the results consistently show higher early morning net radiation and a more rapid CBH increase at Gobabeb, beginning around 05:00 h (near sunrise). These patterns highlight stronger insolation and faster surface heating at the inland site, supporting the hypothesis that enhanced radiative input drives quicker inland CBH lifting. Additionally, the intrusion of near-surface easterly winds carrying dry air can enhance the evaporation of fog droplets, leading to cloud thinning and a subsequent rise in CBH. Overall, the results presented and the accompanying discussion underscore the significance of these findings for understanding fog dynamics in this unique coastal environment. However, a detailed attribution of the processes driving the observed CBH changes remains beyond the scope of this study.

3.3 Estimated CBH

CBH is a critical parameter for the spatial occurrence of fog, and a necessary observable for its spatial mapping. However, due to the sparsity of the direct measurements of CBH (Figure 2), climatological fog mapping is not possible using ceilometer data alone. This is the motivation to test with what accuracy CBH can be estimated from meteorological measurements (RH) that are available for a longer time period and at more locations. Figure 8 presents density scatter plots illustrating the relationship between CBH and surface RH at two representative stations: Coastal Met (Figure 8(a)) and Gobabeb (Figure 8(b)). A notable finding from these plots is the pronounced inverse relationship between CBH and RH, indicating that lower cloud bases are generally associated with higher near-surface humidity. This relationship supports the physical understanding that elevated RH near the surface facilitates fog or low cloud formation by reducing the lifting condensation level. Quantile regression is

https://doi.org/10.5194/egusphere-2025-2645
Preprint. Discussion started: 22 July 2025

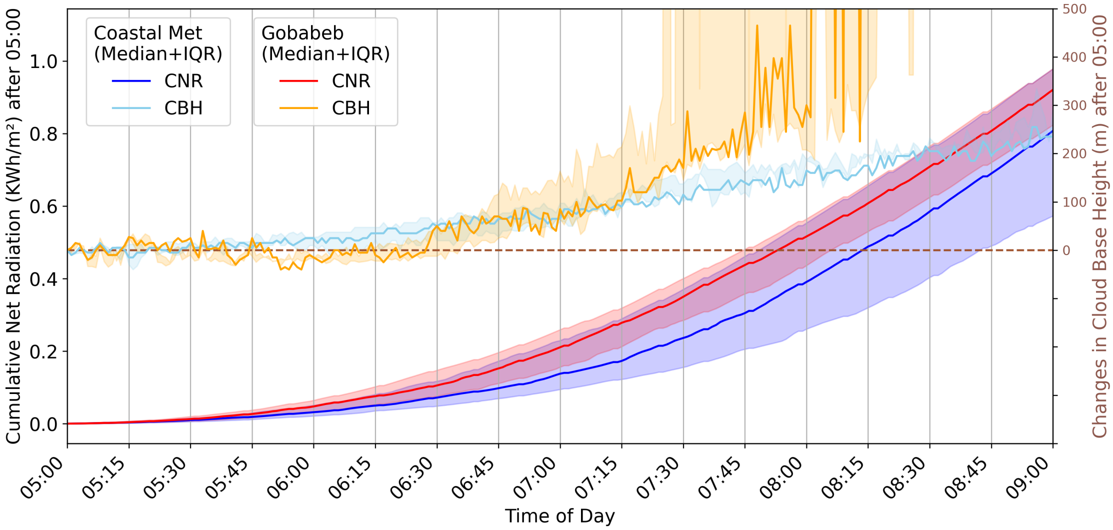

Figure 7. Early morning evolution of cumulative net radiation (CNR) and cloud base height (CBH) from 05:00 to 09:00 during September to December 2017, for cases with cloud presence at both Gobabeb (GB) and Coastal Met (CM). CBH values are reduced to 0 m at 05:00 to highlight relative changes. Shading denotes the interquartile range (IQR) around the median.

applied within a restricted RH range (80–95 %, marked in red color), where RH is less affected by instrumental biases at higher humidity, and where the distribution of CBH residuals is possible above and below the fitted line.

Figure 8(a) shows the relationship between CBH and RH is characterized by a linear and strong negative correlation (Pearson r = 0.71), indicating that increases in RH are generally associated with a decrease in CBH. This aligns well with physical expectations, as higher surface humidity levels facilitate fog formation and sustain lower cloud bases. Such a relationship is consistent with the characteristics of a well-mixed boundary layer (Wood and Bretherton, 2004). The quantile regression of the median (0.5 quantile) yields a slope of -22.1 m/%, meaning that for every 1 % increase in near-surface RH, the predicted median CBH decreases by approximately 22 m. The mean absolute error and mean absolute percentage error are approximately 47 m and 19 %, respectively, both calculated by comparing the estimated CBH with ceilometer observations at the Coastal Met station. Examining the Coastal Met CBH histogram, a bimodal distribution is apparent, with peaks around 310 m and 170 m, which may reflect CBH seasonality, corresponding to the High-FLC and Low-FLC seasons, respectively. Notably, the ceilometer has a detection limit of CBH at 40 m (Preissler et al., 2024), which closely aligns with the quantile regression model's prediction of 44.3 m at 100 % RH. As the CBH-RH relationship is linear even at RH $>$ 95 %, this likely points to a general bias in the ceilometer-based CBH measurements (overestimation of $\sim$ 40 m). At Gobabeb, the relationship between CBH and RH closely resembles that observed at Coastal Met, as evidenced by the Pearson correlation coefficient of 0.78, a mean absolute error of 39.8 m, and a quantile regression slope of -23 m/%. This shows that the RH-CBH relationship is qualitatively and quantitatively consistent at a regional scale. However, two aspects are different between these two locations:

https://doi.org/10.5194/egusphere-2025-2645
Preprint. Discussion started: 22 July 2025

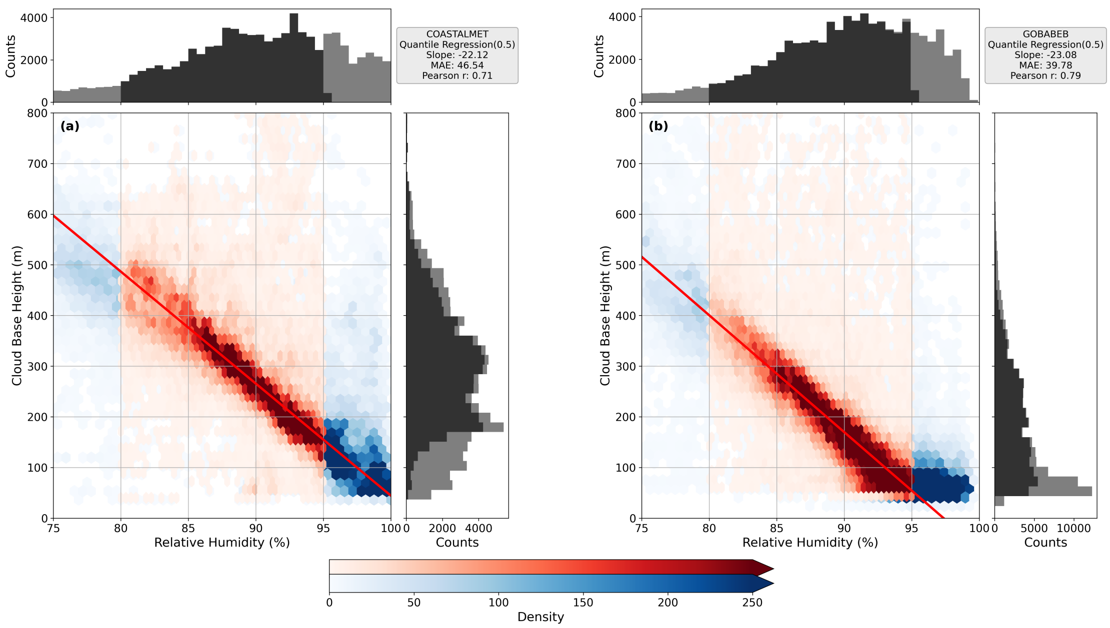

Figure 8. Density scatter plots showing the relationship between CBH and RH for two stations: (a) Coastal Met and (b) Gobabeb. Red shades highlight the RH range between 80 % and 95 %, which is used for the 0.5 quantile regression fit, shown as a solid red line. Marginal histograms along the top and right axes show the distribution of RH and CBH, respectively, the black shade correspond to data within the 80–95 % RH range and their associated CBH values.

1) the point cloud and regression fit are notably shifted (i.e. in Gobabeb the same CBH occurs at lower RH than in CM), and 2) the RH-CBH relationship is not linear at humidities exceeding ~ 95 %. As shown in the RH histogram, in Gobabeb humidity rarely reaches values close to 100 %, even in situations where the stratus is directly at the surface. The quantile regression predicts a CBH of 0 m at RH of 97.5 %. It is therefore likely that these discrepancies can be largely attributed to measurement uncertainties at high humidities and a possible dry bias of the RH measurements. The CS215 sensor that measures RH in Gobabeb is observed to feature a drift over time towards measuring decreasing RH values during fog events (see Appendix Figure A1). Despite these measurement uncertainties, the consistency in the CBH-RH relationship at Gobabeb (particularly within the 80–95 % RH range) indicates that the underlying CBH-RH physical relationship remains consistent with that at Coastal Met.

The quantile regression trained on Coastal Met data was applied to estimate a cloud base height (CBH_e) using the entire RH time series from all FogNet stations. Figure 9 shows the density distributions of RH and CBH_e during satellite observed FLC events and during fog events observed through FogNet measurements. Across all stations except Gobabeb (GB) and Garnet Koppie (GK), nearly all fog events exhibit an RH > 98 %, and peaking near 100 %, which is expected during fog. CBH_e values predicted with the quantile regression are therefore around 50–70 m AGL in fog situations due to the 44.3 m bias. At Garnet Koppie and even more pronounced at Gobabeb, however, RH during fog is lower, peaking at 97.5 % in Gobabeb. CBH_e

https://doi.org/10.5194/egusphere-2025-2645
Preprint. Discussion started: 22 July 2025

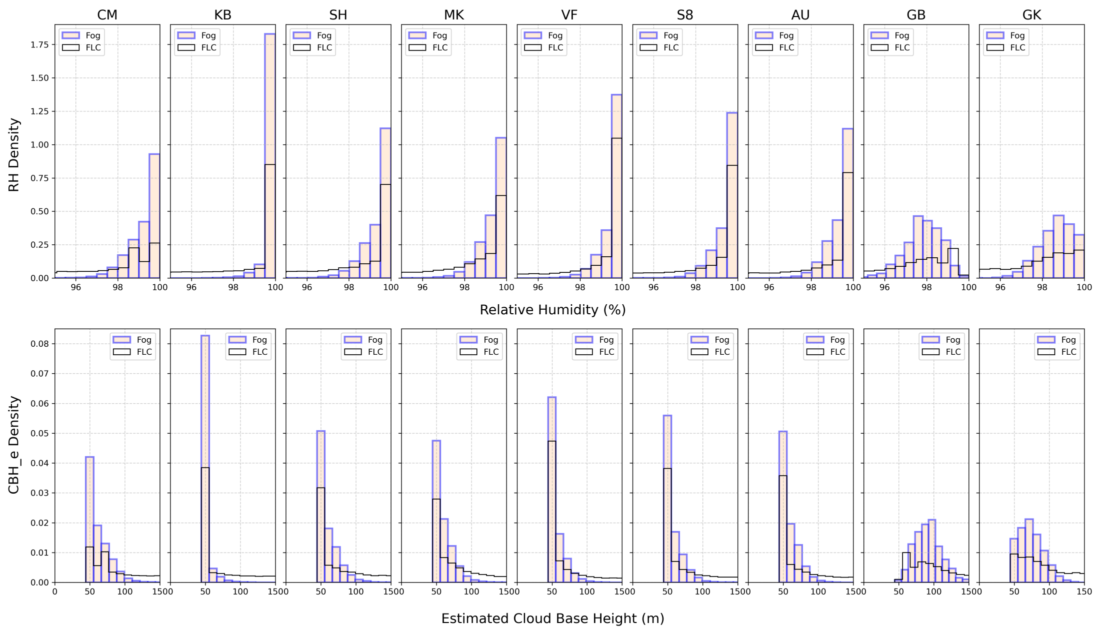

Figure 9. Density histograms of RH (upper panel) and (CBH_e) (bottom panel) during fog event and satellite derived fog and low cloud (FLC) occurrences across different FogNet stations.

therefore also peaks at 70 m or 100 m, respectively. This systematic shift can be attributed to a dry bias likely caused by sensor drift or degradation at these sites (see Appendix figure A1). The CBH_e distribution during satellite-derived FLC occurrences follows a similar pattern but includes lower RH values and exhibits a broader spread toward higher CBH_e values, as it also includes situations where the stratus is lifted from the ground. In other words, this means that fog, as measured at the ground, is associated with very high RH and very low CBH_e, whereas satellite-observed FLC includes both fog and low stratus clouds that may be elevated above the surface, resulting in broader distributions of RH and CBH_e.

3.3.1 A case study

Figure 10 provides an overview of the temporal evolution of CBH_e at a subset of FogNet stations during a representative fog event during the night of 27–28 September 2017, also studied in Spirig et al. (2019). In the figure, CBH_e is shown as above-ground level (AGL) (panel a) and above mean sea level (AMSL) (panel b). In the figure, CBH_e is shown as a dashed line whenever the satellite suggests clear sky, and a solid line when the satellite has detected FLCs. Grey shade indicates whenever in-situ station measurements suggest fog occurrence. During the event, CBH_e values at Coastal Met show a lifted stratus between 200 and 300 m AGL (94 m at CM, top panel), closely aligning with ceilometer observations (dashdot magenta line). Notably, the ceilometer signal shows no lowering and little lifting of CBH during the event. At inland stations (e.g. VF, AU, GB and GK), the stratus is advected close to the surface, with CBH_e values indicating a slight lowering at the start of the

https://doi.org/10.5194/egusphere-2025-2645
Preprint. Discussion started: 22 July 2025

event. When stations suggest that the stratus touches the ground, CBH_e is constant at around 40 m for all stations but Gobabeb and Garnet Koppie, where RH (and therefore CBH_e) converges slowly to its minimum. The panel (b) showing CBH_e AMSL provides further insight into the altitudinal distribution of CBH_e across stations relative to mean sea level. At near-coastal locations where the stratus remains lifted from the ground (CM), CBH_e is consistently around 400 m AMSL, corresponding to the typical stratus deck height observed in the region during this time of year (Andersen et al., 2019). In contrast, at stations further inland where the stratus reaches the surface, CBH_e varies between 450 and 850 m AMSL during fog. The stratus is therefore at least 400 m thick (annotated as Minimum Cloud Thickness in Figure 10(b), suggesting that the CBH_e at Garnet Koppie is likely within the stratus, potentially near its upper boundary. It should be noted that prior to the fog event in Garnet Koppie and shortly after it, the CBH_e of $>$1000 m indicates dry conditions (RH of around 50%), underscoring that the advected stratus is a completely different air mass that replaces the dry continental air masses that are present before the fog event and leads to an RH jump of 40-50% in the matter of minutes. At the end of the fog event, the development of CBH_e suggests a lifting of the FLC layer that is more rapid at inland locations than close to the coast, agreeing with the ceilometer observations and lifting rates presented in section 3.2. The results show that CBH_e can accurately capture the spatial patterns of vertical FLC evolution, and can be used in the future to separate fog from lifted stratus in satellite-based FLC products.

4 Conclusions and outlook

This study addresses key knowledge gaps in understanding the vertical structure of advected stratus in the Central Namib. Using ceilometer observations, it provides a comprehensive analysis of the patterns and variability of the fog/stratus base altitude at coastal and inland locations in the Central Namib Desert, and develops an approach to estimate CBH from near-surface relative humidity measurements. The findings support the study's objectives by offering new insights into fog life cycle processes and enabling region-wide CBH estimation across the FogNet network. The main findings are:

- The study confirms a distinct seasonal cycle of CBH, with lower cloud bases during peak fog seasons at both coastal and inland sites, consistent with earlier work by (Andersen et al., 2019). Superimposed on this seasonal pattern is a pronounced diurnal cycle of CBH, particularly at inland locations. While the CBH at the coastal site of Swakopmund exhibits only a weak diurnal cycle, sites further inland such as Coastal Met (17 km from the coast) and Gobabeb (56 km inland) show a pattern of nighttime CBH lowering and lifting after sunrise. These diurnal patterns of CBH have implications for the spatial distribution of fog during its life cycle.

- A quantitative measure of CBH lowering/lifting rates is developed on the basis of a rolling window regression of the CBH time series. The nighttime CBH lowering is shown to be moderate at rates of 10–50 m h^{-1}, while the lifting is more rapid at 30–150 m h^{-1}, with stronger lifting observed inland at Gobabeb. A delay of CBH lowering is observed at inland sites and is indicative of the inland progression of a stratus layer that features a gradient in thickness near the cloud edge. The more rapid lifting at inland sites may be caused by a thinner inland stratus enabling faster dissipation via enhanced surface heating. A quantitative measure of CBH lowering/lifting rates has been missing in the literature

https://doi.org/10.5194/egusphere-2025-2645
Preprint. Discussion started: 22 July 2025

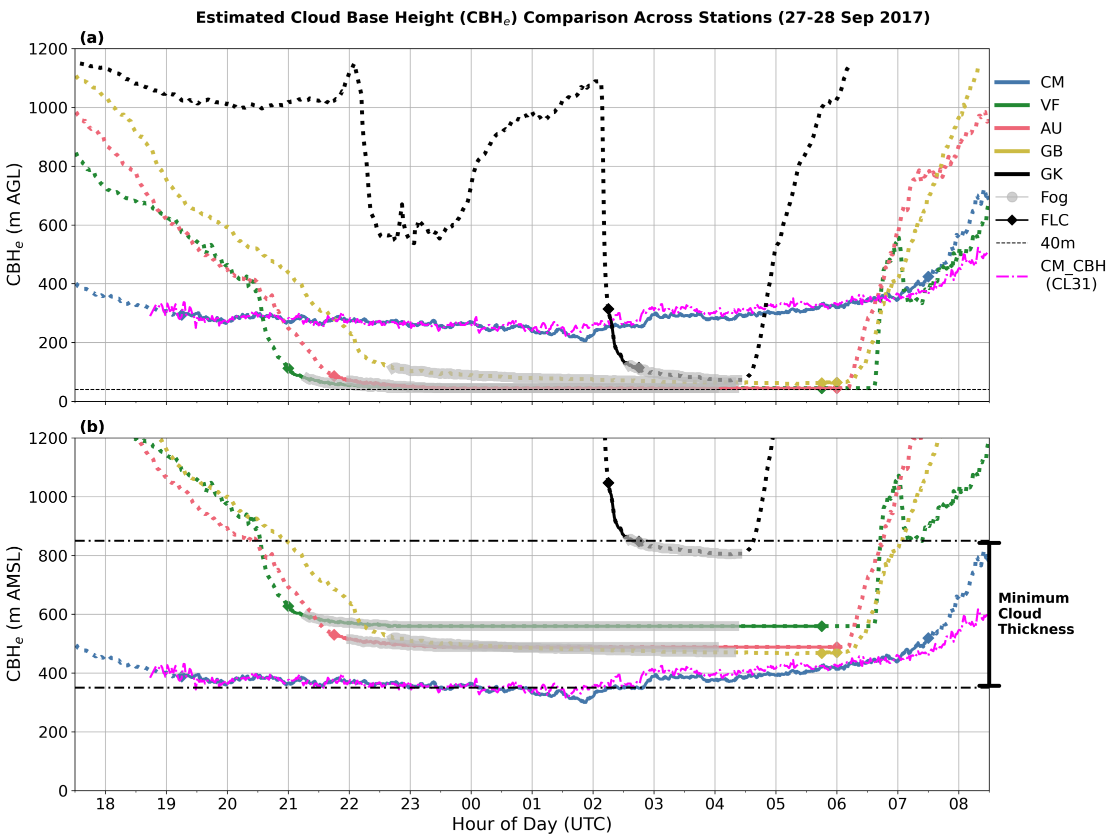

Figure 10. CBH$_e$ at five selected FogNet stations during a representative fog event on 27-28 September 2017 (stations selected for regional representativeness and figure clarity). Each curve (color-coded) corresponds to one station, with dashed and solid line styles indicating satellite-derived clear-sky and FLC conditions, respectively. Diamond markers denote the start and end times of satellite-detected FLC, while grey markers indicate ground-observed fog occurrences. The vertical bar in panel (b) illustrates the potential cloud thickness during the event.

where stratus lowering and lifting is only described anecdotally (Dupont et al., 2016; Wærsted et al., 2019; Toledo et al., 2021; Fathalli et al., 2022; Dione et al., 2023; Singh et al., 2024).

– A robust negative linear relationship is found at both Coastal Met and Gobabeb, with the Pearson's correlation coefficients of -0.71 and -0.78, respectively. This relationship indicates that the stratus clouds form within a well-mixed marine boundary layer and are advected inland, where they can manifest as fog upon interaction with local topography. A quantile regression model trained on RH successfully estimates CBH with a mean absolute error of 46 m. Measurement uncertainties, including RH sensor drift and ceilometer detection thresholds, are likely the main cause of CBH estimation uncertainties. The model also assumes linearity in the RH–CBH relationship, which may not hold in all situations.

https://doi.org/10.5194/egusphere-2025-2645
Preprint. Discussion started: 22 July 2025

- The quantile regression model enables estimation of cloud base height across the FogNet network, extending CBH information beyond the ceilometer sites. In a representative case study, the CBH_e can accurately capture the spatial patterns of vertical FLC evolution providing an estimate of the regional cloud field. The increase in CBH_e with distance inland reflects the thinning of the stratus layer toward its edge.

Future research can leverage this new decade-long CBH_e dataset for the FogNet network and existing satellite products for CBH-based separation of fog from lifted stratus clouds in existing satellite-based FLC products (e.g., Andersen and Cermak, 2018), which can facilitate the development of the first spatially coherent fog maps for the Central Namib and lays the groundwork for long-term fog climatologies. The new measure of CBH lowering/lifting rates enables analyses of the processes driving vertical development of stratus bases. Taken together, our findings have important implications for enhancing our understanding of fog life cycle mechanisms, and for quantifying fog-related deposition of water, nutrients, and pollutants, as well as their impacts on the regional desert ecosystem.

Appendix A

Figure A1

Code and Data Availability

Ceilometer and FogNet data are observational datasets collected from multiple sites and are available from the corresponding authors upon reasonable request. The satellite-based Fog and Low Cloud (FLC) data can be accessed upon request via the source described in Andersen and Cermak (2018). The code used for data processing and analysis is also available from the corresponding authors upon reasonable request.

Author Contributions

DM, HA, and JC conceived the idea for the analysis. DM carried out the data collection, analysis, and drafted the manuscript. HA contributed to the development of the methodology and the core research. RV supported the data collection. HA, JC, RV, and BA assisted in manuscript preparation and contributed to interpreting the results.

Acknowledgments

Funding for this study was provided by Deutsche Forschungsgemeinschaft (DFG) in the project Aerosols and fog in southern Africa: processes and impact on biogeochemistry (AeroFog). The authors would like to thank the entire AeroFog team, for their assistance during the field campaign in 2024. We thank Anja v.d. Plas and her colleagues from the Ministry of Fisheries and Marine Resources (Swakopmund, Namibia), Mary Seely, and Werner Petrick for the support and for hosting the CL31

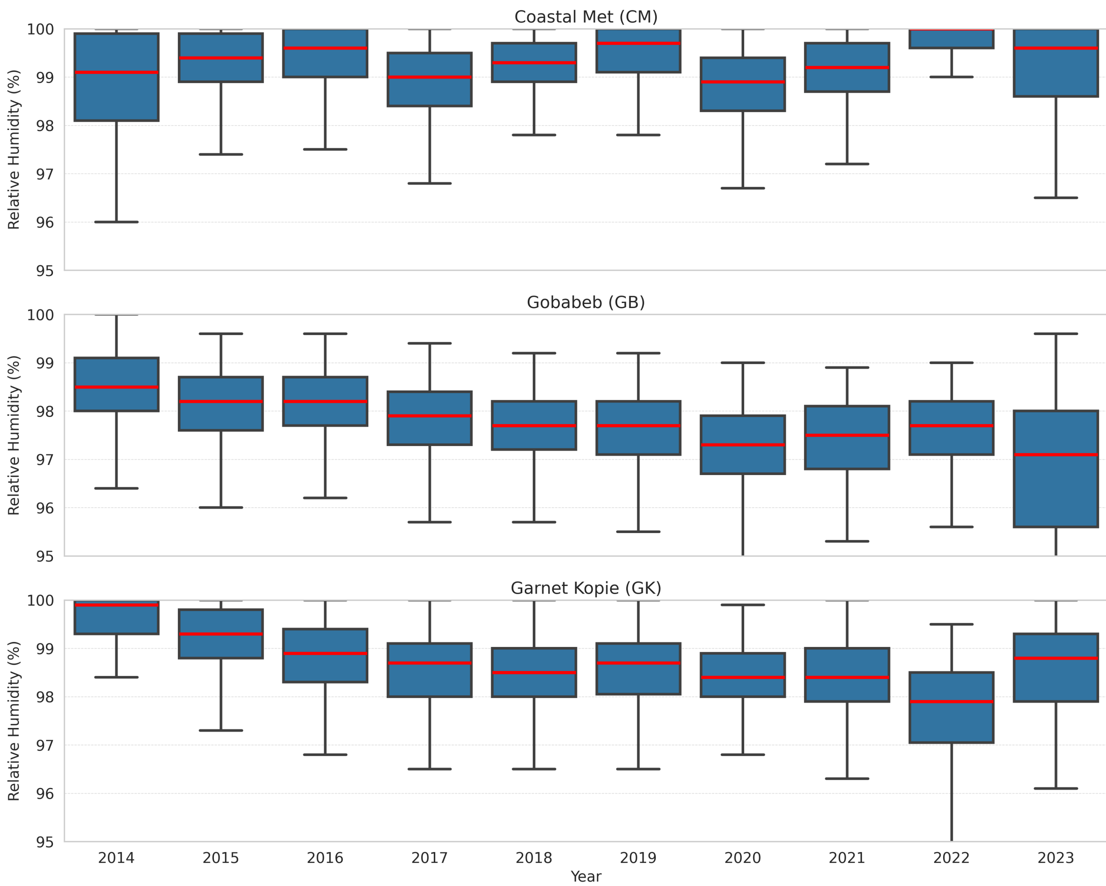

Figure A1. Yearly distribution of Relative Humidity (RH) during fog events at Coastal Met (top), Gobabeb (middle) and Garnet Kopie (bottom) from 2014 to 2023. Boxplots represent the inter-quartile range (IQR), with whiskers extending to 1.5×IQR, and red lines indicating the median.

instrument. The authors also thank Frank Göttsche and Axel Göbel for the maintenance of the CL31 instrument and the
385 support in data aquisition. The statements, findings, conclusions, and recommendations are those of the authors and do not necessarily reflect the views of NOAA or the U.S. Department of Commerce.

Financial Support

This research has been supported by the Deutsche Forschungsgemeinschaft (DFG, grant no. CE 163/14-1, project no. 505800970) and the Agence Nationale de la Recherche (ANR, grant no. ANR-22-CE92-0051) within the project Aerosols and fog in southern Africa: processes and impact on biogeochemistry (AeroFog). The contribution of co-author Bianca Adler was supported by

https://doi.org/10.5194/egusphere-2025-2645
Preprint. Discussion started: 22 July 2025

NOAA cooperative agreement NA22OAR4320151, for the Cooperative Institute for Earth System Research and Data Science (CIESRDS).

https://doi.org/10.5194/egusphere-2025-2645
Preprint. Discussion started: 22 July 2025

References

Andersen, H. and Cermak, J.: First fully diurnal fog and low cloud satellite detection reveals life cycle in the Namib, Atmospheric Measurement Techniques, 11, 5461–5470, 2018.

Andersen, H., Cermak, J., Solodovnik, I., Lelli, L., and Vogt, R.: Spatiotemporal dynamics of fog and low clouds in the Namib unveiled with ground-and space-based observations, Atmospheric Chemistry and Physics, 19, 4383–4392, 2019.

Andersen, H., Cermak, J., Fuchs, J., Knippertz, P., Gaetani, M., Quinting, J., Sippel, S., and Vogt, R.: Synoptic-scale controls of fog and low-cloud variability in the Namib Desert, Atmospheric Chemistry and Physics, 20, 3415–3438, 2020.

Andrews, W. and Hutchings, L.: Upwelling in the southern Benguela Current, Progress in Oceanography, 9, 1–81, 1980.

Azúa-Bustos, A., González-Silva, C., Mancilla, R. A., Salas, L., Gómez-Silva, B., McKay, C. P., and Vicuña, R.: Hypolithic cyanobacteria supported mainly by fog in the coastal range of the Atacama Desert, Microbial Ecology, 61, 568–581, 2011.

Barbato, G., Zollo, A. L., and Mercogliano, P.: Analysis of the planetary boundary layer using CS135 ceilometer, in: 2016 IEEE Metrology for Aerospace (MetroAeroSpace), pp. 124–129, IEEE, 2016.

CampbellScientific: Loggernet user manual, Campbell Scientific, available at: https://s.campbellsci.com/documents/au/manuals/loggernet2-1.pdf, 2007.

CampbellScientific: wind monitor: user manual, Campbell Scientific, available at: https://s.campbellsci.com/documents/us/miscellaneous/old-manuals/05103,%2005103-45,%2005106,%2005108,%2005108-45,%20and%2005305%20Wind%20Monitors.pdf, 2013a.

CampbellScientific: CS215 temp and rh probe: user manual, Campbell Scientific, available at: https://s.campbellsci.com/documents/ca/manuals/cs215_man.pdf, 2013b.

CampbellScientific: CNR4 net radiometer: user manual, Campbell Scientific, available at: https://s.campbellsci.com/documents/ca/manuals/cnr4_man.pdf, 2017.

CampbellScientific: CS135 Ceilometer: user manual, Campbell Scientific, available at: https://s.campbellsci.com/documents/eu/manuals/cs135.pdf, 2018.

Cermak, J.: Low clouds and fog along the South-Western African coast—Satellite-based retrieval and spatial patterns, Atmospheric Research, 116, 15–21, 2012.

Cermak, J.: Fog and low cloud frequency and properties from active-sensor satellite data, Remote Sensing, 10, 1209, 2018.

Cermak, J. and Bendix, J.: Detecting ground fog from space–a microphysics-based approach, International Journal of Remote Sensing, 32, 3345–3371, 2011.

Dione, C., Haeffelin, M., Burnet, F., Lac, C., Canut, G., Delanoë, J., Dupont, J.-C., Jorquera, S., Martinet, P., Ribaud, J.-F., et al.: Role of thermodynamic and turbulence processes on the fog life cycle during SOFOG3D experiment, Atmospheric Chemistry and Physics, 23, 15 711–15 731, 2023.

Dupont, J., Haeffelin, M., Stolaki, S., and Elias, T.: Analysis of dynamical and thermal processes driving fog and quasi-fog life cycles using the 2010–2013 ParisFog dataset, Pure and Applied Geophysics, 173, 1337–1358, 2016.

Dupont, J.-C., Haeffelin, M., Protat, A., Bouniol, D., Boyouk, N., and Morille, Y.: Stratus–fog formation and dissipation: a 6-day case study, Boundary-layer meteorology, 143, 207–225, 2012.

Ebner, M., Miranda, T., and Roth-Nebelsick, A.: Efficient fog harvesting by Stipagrostis sabulicola (Namib dune bushman grass), Journal of arid environments, 75, 524–531, 2011.

Eckardt, F., Soderberg, K., Coop, L., Muller, A., Vickery, K., Grandin, R., Jack, C., Kapalanga, T., and Henschel, J.: The nature of moisture at Gobabeb, in the central Namib Desert, Journal of arid environments, 93, 7–19, 2013.

Egli, S., Thies, B., and Bendix, J.: A hybrid approach for fog retrieval based on a combination of satellite and ground truth data, Remote Sensing, 10, 628, 2018.

Fathalli, M., Lac, C., Burnet, F., and Vié, B.: Formation of fog due to stratus lowering: An observational and modelling case study, Quarterly Journal of the Royal Meteorological Society, 148, 2299–2324, 2022.

Formenti, P., D'Anna, B., Flamant, C., Mallet, M., Piketh, S. J., Schepanski, K., Waquet, F., Auriol, F., Brogniez, G., Burnet, F., et al.: The aerosols, radiation and clouds in southern Africa field campaign in Namibia: Overview, illustrative observations, and way forward, Bulletin of the American Meteorological Society, 100, 1277–1298, 2019.

Gan, H. Y., Hohberg, K., Schneider, C., Ebner, M., Marais, E., Miranda, T., Lehmitz, R., Maggs-Kölling, G., and Bocherens, H.: The hidden oases: unveiling trophic dynamics in Namib's fog plant ecosystem, Scientific Reports, 14, 13 334, 2024.

Gottlieb, T. R., Eckardt, F. D., Venter, Z. S., and Cramer, M. D.: The contribution of fog to water and nutrient supply to Arthraerua leubnitziae in the central Namib Desert, Namibia, Journal of Arid Environments, 161, 35–46, 2019.

Juvik, J. O. and Nullet, D.: Comments on" A Proposed Standard Fog Collector for Use in High-Elevation Regions", Journal of Applied Meteorology (1988-2005), 34, 2108–2110, 1995.

Kaspar, F., Helmschrot, J., Mhanda, A., Butale, M., De Clercq, W., Kanyanga, J., Neto, F., Kruger, S., Castro Matsheka, M., Muche, G., et al.: The SASSCAL contribution to climate observation, climate data management and data rescue in Southern Africa, Advances in science and research, 12, 171–177, 2015.

Koenker, R. and Hallock, K. F.: Quantile regression, Journal of economic perspectives, 15, 143–156, 2001.

Lancaster, J., Lancaster, N., and Seely, M.: Climate of the Central Namib Desert, Madoqua, 14, 5–61, 1984.

Mass, A., Andersen, H., Cermak, J., Formenti, P., Pauli, E., and Quinting, J.: A satellite-based analysis of semi-direct effects of biomass burning aerosols on fog and low cloud dissipation in the Namib Desert, EGUsphere, 2024, 1–25, 2024.

Maúre, G., Pinto, I., Ndebele-Murisa, M., Muthige, M., Lennard, C., Nikulin, G., Dosio, A., and Meque, A.: The southern African climate under 1.5 C and 2 C of global warming as simulated by CORDEX regional climate models, Environmental Research Letters, 13, 065 002, 2018.

McHugh, T. A., Morrissey, E. M., Reed, S. C., Hungate, B. A., and Schwartz, E.: Water from air: an overlooked source of moisture in arid and semiarid regions, Scientific Reports, 5, 13 767, 2015.

Nagel, J.: Fog precipitation at Swakopmund, Weather Bureau Newsletter, 125, 1–9, 1959.

Olivier, J.: Some spatial and temporal aspects of fog in the Namib, 1992.

Olivier, J.: Spatial distribution of fog in the Namib, Journal of Arid Environments, 29, 129–138, https://doi.org/https://doi.org/10.1016/S0140-1963(05)80084-9, 1995.

Olivier, J. and Stockton, P. L.: The influence of upwelling extent upon fog incidence at Lüderitz, southern Africa, International Journal of Climatology, 9, 69–75, https://doi.org/https://doi.org/10.1002/joc.3370090106, 1989.

Pilié, R., Mack, E., Rogers, C., Katz, U., and Kocmond, W.: The formation of marine fog and the development of fog-stratus systems along the California coast, Journal of Applied Meteorology (1962-1982), pp. 1275–1286, 1979.

Pope, N. H. and Igel, A. L.: Counteracting Influences of Gravitational Settling Modulate Aerosol Impacts on Cloud Base Lowering Fog Characteristics, EGUsphere, 2024, 1–18, https://doi.org/10.5194/egusphere-2024-3214, 2024.

Preissler, J., O'Connor, E., Kayser, M., Hervo, M., Lehmann, V., Toupoint, C., Holst, C. C., Gryning, S.-E., Batchvarova, E., Céspedes, J., et al.: JND European networks observing the atmospheric boundary layer: Overview, access and impacts: Chapter: Doppler lidar (DL), 2024.

Qiao, N., Wang, L., Marais, E., and Li, F.: Fog detection and estimation using CALIPSO lidar observations, Geophysical Research Letters, 49, e2022GL101 375, 2022.

Roth-Nebelsick, A., Ebner, M., Miranda, T., Gottschalk, V., Voigt, D., Gorb, S., Stegmaier, T., Sarsour, J., Linke, M., and Konrad, W.: Leaf surface structures enable the endemic Namib desert grass Stipagrostis sabulicola to irrigate itself with fog water, Journal of the Royal Society interface, 9, 1965–1974, 2012.

Seely, M. and Henschel, J.: The climatology of Namib fog, 1998.

Shanyengana, E., Henschel, J., Seely, M., and Sanderson, R.: Exploring fog as a supplementary water source in Namibia, Atmospheric Research, 64, 251–259, 2002.

Singh, D. K., Hoch, S. W., Gultepe, I., and Pardyjak, E. R.: A case study of the life cycle of a stratus-lowering coastal-fog event in Newfoundland, Canada, Quarterly Journal of the Royal Meteorological Society, 150, 641–662, 2024.

Spirig, R., Vogt, R., Larsen, J. A., Feigenwinter, C., Wicki, A., Franceschi, J., Parlow, E., Adler, B., Kalthoff, N., Cermak, J., et al.: Probing the fog life cycles in the Namib Desert, Bulletin of the American Meteorological Society, 100, 2491–2507, 2019.

Toledo, F., Haeffelin, M., Wærsted, E., and Dupont, J.-C.: A new conceptual model for adiabatic fog, Atmospheric Chemistry and Physics Discussions, 2021, 1–32, 2021.

Vaisala: CL31 Ceilometer: user manual, Vaisala, available at: https://docs.vaisala.com/r/M210482EN-L/en-US, 2024.

Wærsted, E. G., Haeffelin, M., Steeneveld, G.-J., and Dupont, J.-C.: Understanding the dissipation of continental fog by analysing the LWP budget using idealized LES and in situ observations, Quarterly Journal of the Royal Meteorological Society, 145, 784–804, 2019.

Wagh, S., Krishnamurthy, R., Wainwright, C., Wang, S., Dorman, C. E., Fernando, H. J., and Gultepe, I.: Study of stratus-lowering marine-fog events observed during C-FOG, Boundary-Layer Meteorology, 181, 317–344, 2021.

Warren-Rhodes, K. A., McKay, C. P., Boyle, L. N., Wing, M. R., Kiekebusch, E. M., Cowan, D. A., Stomeo, F., Pointing, S. B., Kaseke, K. F., Eckardt, F., et al.: Physical ecology of hypolithic communities in the central Namib Desert: the role of fog, rain, rock habitat, and light, Journal of Geophysical Research: Biogeosciences, 118, 1451–1460, 2013.

Weathers, K. C., Ponette-González, A. G., and Dawson, T. E.: Medium, vector, and connector: Fog and the maintenance of ecosystems, Ecosystems, 23, 217–229, 2020.

Weigner, M., Bravo Aranda, J. A., et al.: Aerosol backscatter profiles from ceilometers: validation of water vapor correction in the framework of CeiLinEx2015, 2019.

Wood, R. and Bretherton, C. S.: Boundary layer depth, entrainment, and decoupling in the cloud-capped subtropical and tropical marine boundary layer, Journal of climate, 17, 3576–3588, 2004.

Zivot, E. and Wang, J.: Rolling Analysis of Time Series, pp. 299–346, Springer New York, New York, NY, https://doi.org/10.1007/978-0-387-21763-5_9, 2003.